JOURNAL OF MATERIALS SCIENCE **37** (2002) 2899 – 2907

Creep deformation and monotonic stress-strain behavior of Haynes alloy 556 at elevated temperatures

M. S. ABU-HAIBA, A. FATEMI*, M. ZOROUFI
Department of Mechanical, Industrial and Manufacturing Engineering, The University of Toledo, Toledo, Ohio, USA
E-mail: afatemi@eng.utoledo.edu

Creep and monotonic stress-strain behaviors of Haynes alloy 556 are studied and characterized at elevated temperatures using experimental results and analytical models. The Θ-Projection and Garofalo creep models describe the variations of the creep curve shape at different temperatures and stress levels reasonably well. The Θ-Projection method, however, results in accurate prediction of the rupture lives, while Garofalo model overestimates them. Both models provide fair predictions of minimum creep rate variations with stress at a given temperature. An incremental time method, which combines the time independent stress-strain data from standard tensile test with the creep data, is used to predict the stress-strain curve in slow-strain-rate tensile tests at elevated temperatures.

Nomenclature

C	Power-law breakdown stress
CR	Creep rate at any time, t
CR_i	Initial creep rate
E	Modulus of elasticity
K	Monotonic strain-hardening coefficient
MCR	Minimum creep rate
n	Monotonic strain-hardening exponent, or creep exponent
Q	Activation energy for creep
R	Universal gas constant
R.T.	Room temperature
r	Rate constant for creep
t	Time
T	Temperature
T_t	Transition temperature above which the activation energy is constant
t_m	Time to minimum creep rate
t_R	Rupture time
ε	Total strain
ε_e	Elastic strain
ε_0	Instantaneous strain on loading
ε_p	True plastic strain
ε_R	Rupture strain
ε_t	Limit for the transition creep
Θ_1, Θ_2, Θ_3, Θ_4	Constants of the Θ-Projection model
σ	True stress
τ	Maximum attainable stress rate

1. Introduction

One of the most critical factors determining the structural integrity of elevated temperature components is their creep behavior. Creep at high-temperature can lead to micro-cracking and ultimate fracture and, therefore, is one of the main mechanisms that limits the component life.

Creep properties are generally determined by means of a test in which a constant load or stress is applied to a specimen and the resulting strain is recorded as a function of time. Fig. 1 shows a typical creep curve. After the initial instantaneous strain, a decelerating strain rate stage (transient primary creep) leads to a steady minimum creep rate (*MCR*), which is finally followed by an accelerating stage (tertiary creep) that ends to fracture at a rupture time, t_R. During primary creep, the decreasing slope of the creep curve is attributed to strain hardening. Secondary stage creep is explained in terms of a balance between strain hardening, softening, and damage processes, resulting in a nearly constant creep rate. The tertiary stage is attributed to the appearance of internal or external damage processes coupled with softening processes, resulting in a decrease in the resistance to load or a significant increase in the net sectional stress.

The rupture life, t_R, at a given temperature and stress level is generally obtained when it is necessary to evaluate the response of a material for using in short life situations, such as for rocket engine ($t_R = 100$ sec) or a

*Author to whom all correspondence should be addressed.

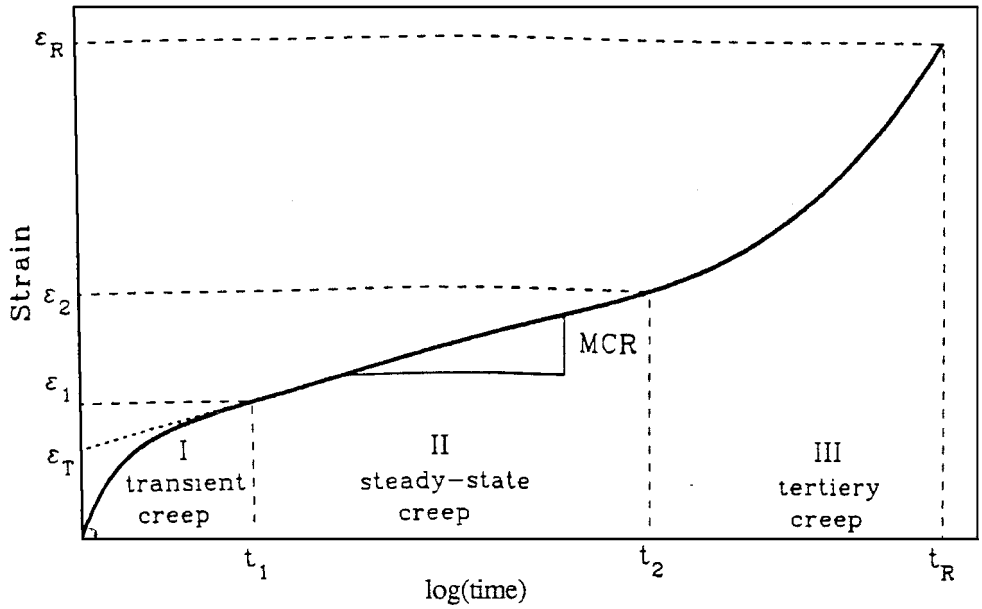

Figure 1 Schematic representation of a typical creep curve.

turbine blade in a military aircraft engine ($t_R = 100$ hrs) [1]. In such short life situations, the major question is whether the component will or will not fail, rather than how much it will deform. As a result, the details of the creep-time curve are not of central importance to the engineering problem.

Over the past several decades, a range of methods have been developed for the prediction and evaluation of creep resistance. The most widely used methods include constitutive equations and parametric correlations. A typical example of constitutive equations is the Θ-Projection method given by:

$$\varepsilon = \varepsilon_0 + \Theta_1\left[1 - e^{(-\Theta_2 t)}\right] + \Theta_3\left[e^{(\Theta_4 t)} - 1\right] \quad (1)$$

where Θ_1, Θ_2, Θ_3, and Θ_4 are constants, which are functions of stress and temperature, and ε_0 is the instantaneous strain on loading. Brown [2] found that Equation 1 could be used to predict long-term rupture lives from relatively short time data.

Another model, which is relatively simple and popular, is the Garofalo model, where the strain-time relation is given by:

$$\varepsilon = \varepsilon_0 + \varepsilon_t(1 - e^{-rt}) + (MCR)t \quad (2)$$

where ε_t is the limit for transient creep, r is a constant relating to the rate of exhaustion of the transient creep, and MCR is the steady state or minimum creep rate. In this paper, the ability of these models to predict the variation of the creep curve shape, minimum creep rate, and the long-term rupture life with varying stress and temperature is examined and compared with the experimental creep curves and data.

The stress-strain response of a material is often described using an equation of the form:

$$\varepsilon = \varepsilon_e + \varepsilon_p = \frac{\sigma}{E} + \left(\frac{\sigma}{K}\right)^{1/n} \quad (3)$$

where K is strain hardening coefficient, and n is strain-hardening exponent. Since components are subjected to different loading rates and operating temperatures, it is very useful to be able to predict variations of the stress-strain curve with temperature and strain rate. In this work, variations of modulus of elasticity, strain hardening exponent, and strain hardening coefficient with temperature are also studied based on data from standard tensile tests. In addition, slow-strain-rate tensile test results at high temperatures are analyzed, since creep plays an important role in the determination of the stress-strain response at high temperatures. The stress-strain curve for the material under investigation at a given temperature and strain rate, is then predicted using a time incremental approach which combines time independent material properties (modulus of elasticity, strength coefficient, and strain hardening exponent) and time dependent creep data. The predicted stress-strain curves are then compared with the experimental curves.

2. Experimental data

Experimental data were obtained for Haynes Alloy 556 at elevated temperature. A piece of two-inch thick mill annealed plate was used to make the specimens. The chemical composition of this material is 21 Ni, 18 Co, 22 Cr, 3 Mo, 2.3 W, 0.68 Ta, 0.16 N, 0.4 Si, 1 Mn, 0.15 Al and 0.13 C (all percent by weight), and the balance is Fe. Mechanical properties of interest including modulus of elasticity, coefficient of thermal expansion, yield and ultimate strengths, and percent elongation at different temperatures are listed in Table I [3]. Both standard and slow-strain-rate tensile tests as well as creep tests were performed. The standard tensile and creep test specimens were 12.70 mm in diameter and 31.75 mm in gage length. The slow-strain-rate tensile specimens were 6.40 mm in diameter and 50.80 mm in gage length. Details of experimental procedure are given in [4]. Fatigue and cyclic performance of this material have been evaluated previously [5].

Five standard tensile tests were performed at temperatures ranging from room temperature to 900°C.

TABLE I Summary of basic mechanical properties for Haynes alloy 556 [3]

Temperature (°C)	Modulus of elasticity (GPa)	Coefficient of thermal expansion (μm/m/°C)	0.2% Yield strength (MPa)	Ultimate strength (MPa)	Elongation in 50.8 mm (%)
R.T.	205	–	376	803	51.4
93	201	14.7	N/A	N/A	N/A
204	194	14.9	N/A	N/A	N/A
316	185	15.1	N/A	N/A	N/A
427	177	15.4	N/A	N/A	N/A
538	168	15.7	211	623	60.3
649	159	16.1	211	573	57.4
760	150	16.4	202	472	52.6
871	144	16.7	192	340	69.1
982	139	17.0	128	212	83.9
1093	N/A	17.1	60	111	95.2

TABLE II Data from standard tensile tests for Haynes alloy 556 [4]

Temperature (°C)	0.2% Yield strength (MPa)	Ultimate strength (MPa)	Elongation (%)	Reduction in area (%)	Strain hardening exponent, n	Strain hardening coefficient, K (MPa)
R.T.	414	826	57.0	65.8	0.1168	448
300	265	662	54.0	59.9	0.1299	298
760	214	364	92.0	73.4	0.0931	234
800	220	517	52.8	62.2	0.0773	234
900	202	215	96.8	78.3	0.0137	203

TABLE III Slow-strain-rate tensile data [4]

Temperature (°C)	Modulus of elasticity (GPa)	0.2% Yield strength (MPa)	Flow stress (MPa)	Strain hardening exponent, n	Strain hardening coefficient, K (MPa)
R.T.	200	367	N/A	0.0870	632
316	200	270	N/A	0.1138	548
593	152	225	N/A	0.1090	444
760	140	220	239	0.0332	267
816	133	143	150	0.0229	166
871	111	98.9	104	0.0374	126

TABLE IV Creep data at various temperatures [4]

Temperature (°C)	Stress (MPa)	*MCR* (%/hr)	Time to 1% creep (hrs)	Rupture life (hrs)	Elongation, (%)	Reduction in area (%)
800	40	5.16×10^{-3}	>10,000	N/A	N/A	N/A
800	70	5.59×10^{-4}	1,400	10,652	25.36	31.56
800	100	4.36×10^{-3}	1,500	1,035	43.68	53.39
871	40	7.39×10^{-5}	9,500	N/A	N/A	N/A
760	100	9.03×10^{-4}	400	5,755	21.44	29.51

Typical data from these tests are listed in Table II. Slow-strain-rate tensile tests were also run for temperatures ranging from room temperature to 871°C at a strain rate of 0.5%/hour. Data collected from the slow-strain-rate tensile tests are listed in Table III. Creep tests were run in a lever-arm creep-testing machine at temperatures ranging from 760°C to 871°C. Data from these tests are listed in Table IV.

3. Creep behavior

3.1. Θ-Projection Method

The changes in the creep curve shape with stress and temperature can be described using Equation 1 [6, 7]. Creep rate is determined by differentiating this equation with respect to time:

$$\frac{d\varepsilon}{dt} = \Theta_1\Theta_2 e^{(-\Theta_2 t)} + \Theta_3\Theta_4 e^{(\Theta_4 t)} \quad (4)$$

The first term of the creep rate decreases with time, which is attributed to strain hardening. The second term increases with time, which is attributed to strain softening and damage processes. Equation 1 is based on the concept that two relaxation-type processes, strain hardening (the second term) and strain weakening (the third term), proceed independently during creep, and that a steady-state does not exist in creep of practical materials [6].

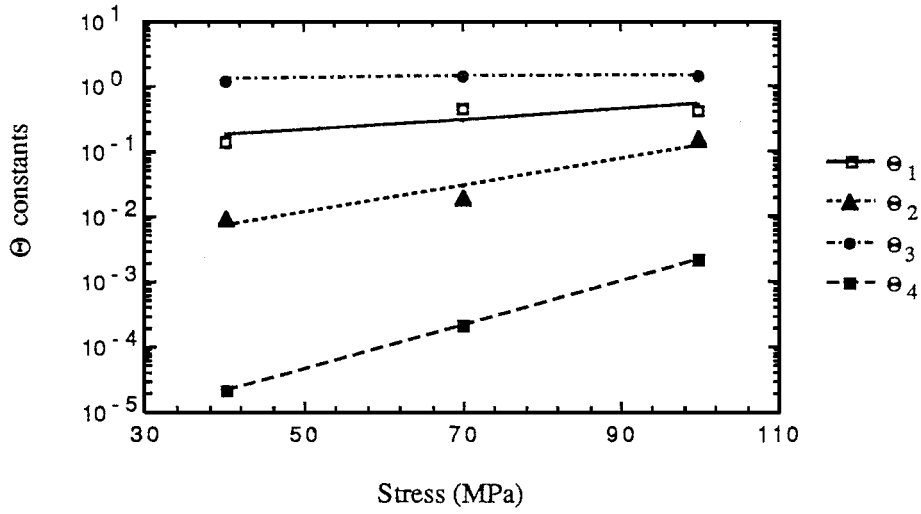

Figure 2 The stress dependence of the Θ constants for the Haynes alloy 556 at 800°C.

The time at which creep rate is minimum is obtained by differentiating Equation 4 with respect to time and setting it equal to zero. The time to minimum creep rate is then found to be:

$$t_m = \frac{1}{\Theta_2 + \Theta_4} \ln \frac{\Theta_1(\Theta_2)^2}{\Theta_3(\Theta_4)^2} \tag{5}$$

The four Θ constants are determined using a non-linear optimization technique which applies the least squares method to the creep equation. The values of the four Θ constants obtained are based on lives ranging from 800 to 5000 hours and their variations with stress level are shown in Fig. 2. This figure suggests linear dependence on stress level in semi-log coordinates. Variation of Θ values with temperature at constant stress could not be obtained based on the available creep data, since only two data points were available at a given stress level. However, analysis of several other materials including 1/2CrMoV, 1CrMoV, 9CrMoVNb, and 12CrMoVNb steels [8] showed that the variations of $\log(\Theta_i)$ with temperature at a constant stress exhibit a linear trend. Accordingly, it is assumed that $\log(\Theta_i)$ varies linearly with stress at a constant temperature, and with temperature at a constant stress level. This can be mathematically represented by an equation of the form:

$$\log(\Theta_i) = a_i + b_i T + c_i \sigma + d_i \sigma T \tag{6}$$

where a_i, b_i, c_i, and d_i are constants determined by the least squares method for each Θ. Fig. 3 shows superimposed plots of experimental and predicted creep curves by the Θ-Projection model (Equation 1). The model fits the experimental results reasonably well within the experimental range.

To examine the ability of the Θ-Projection method to predict long term creep performance from short term data, the rupture lives were calculated using Equation 1 and compared with the experimental rupture lives available for lives up to 10,652 hours. The available experimental rupture strains are given in Table IV as a function of stress and temperature. Using Equation 1, with $\varepsilon_0 = 0$ and $\varepsilon = \varepsilon_r$, where ε_r is the rupture strain, a numerical solution for the rupture life can then be obtained with results shown in Table V. As can be seen, this method gives a fairly good prediction of rupture lives when compared to experimental long-term data of the Haynes alloy 556, but somewhat overestimating the long-term creep performance. Using Equations 4–6 in conjunction with the values of the constants a, b, c, and d, the minimum creep rate for stress levels between 20 MPa and 100 MPa at 800°C were predicted and compared with experimental minimum creep rates in Fig. 4.

3.2. Garofalo model

According to this model, creep curve is represented by the strain-time relation in Equation 1. A relation, which describes the stress dependence of the minimum creep rate at a given temperature, can be described by [9]:

$$MCR = A_1 \mathrm{Sinh}^n(\alpha\sigma) \tag{7}$$

where A_1, n, and α are constants. Since creep is a thermally activated process, its temperature sensitivity

TABLE V Rupture lives as predicted by the Θ-Projection and Garofalo models versus experimental rupture lives

			Θ-Projection model		Garofalo model	
Stress (MPa)	Temperature (°C)	Experimental rupture life (hrs)	Predicted rupture life (hrs)	Predicted to experimental	Predicted rupture life (hrs)	Predicted to experimental
100	760	5,755	5,698	0.99	14,300	2.48
70	800	10,652	14,209	1.33	55,500	5.21
100	800	1,500	1,659	1.11	13,825	9.22

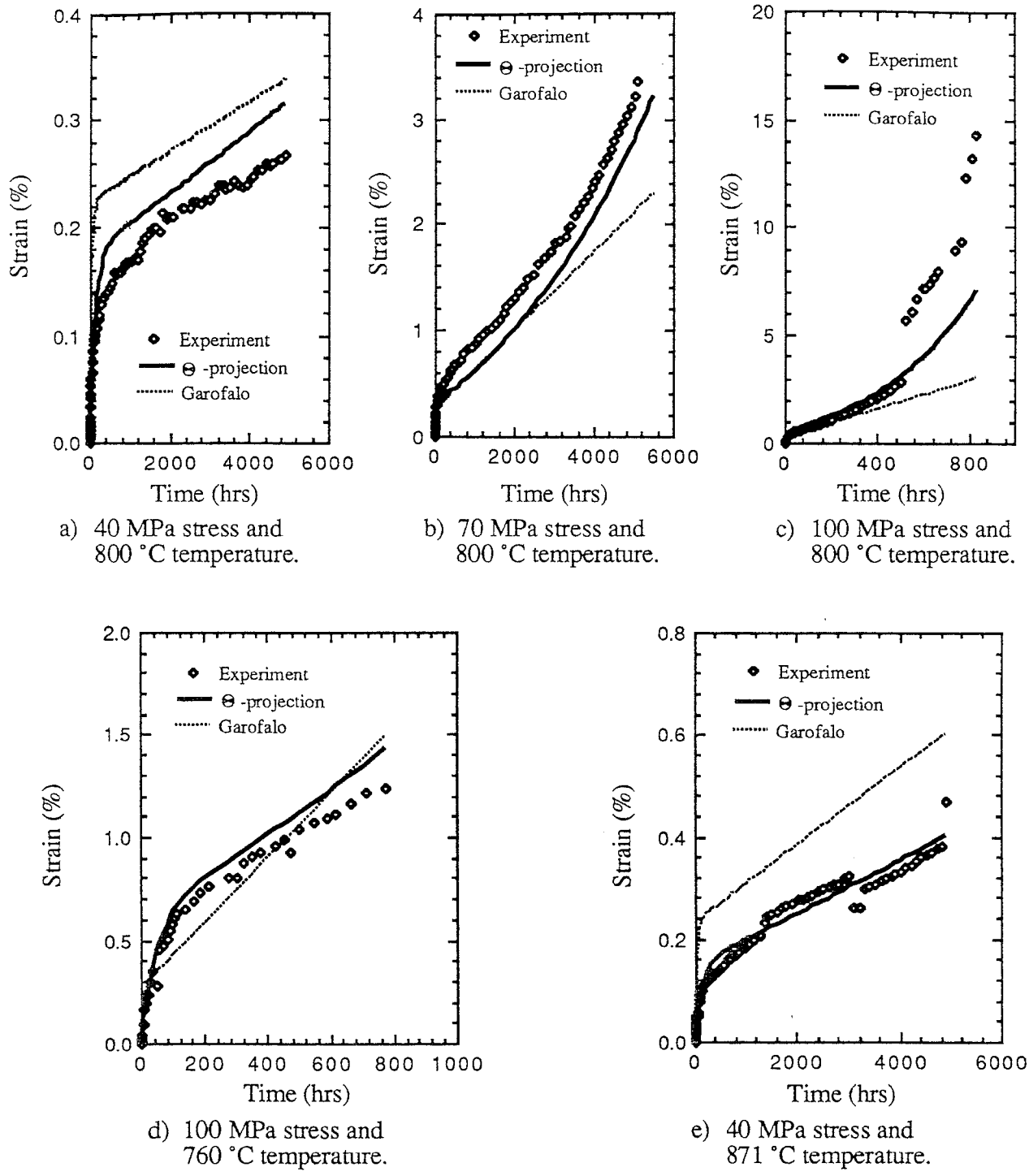

Figure 3 Experimental and predicted creep curves by Θ-Projection and Garofalo models at different temperatures and stress levels.

obeys an Arrhenius-type expression. With characteristic activation energy, Q, for the rate controlling mechanism, the creep rate can be expressed by:

$$MCR = A_2 e^{-Q/RT} \tag{8}$$

where A_2 is a constant and R is the universal gas constant. Combining Equation 7 with Equation 8 results in [10]:

$$MCR = A e^{-Q/RT} \mathrm{Sinh}^n(\alpha\sigma) \tag{9}$$

The values of ε_t, r, and MCR for the creep tests are obtained from the least squares fit of the experimental data to Equation 2. By differentiating Equation 2 with respect to time, one obtains:

$$CR = \varepsilon_t r e^{(-rt)} + MCR \tag{10}$$

where CR is the creep rate at any time t. The initial creep rate, CR_i, at $t = 0$ becomes:

$$CR_i = \varepsilon_t r + MCR \tag{11}$$

A plot of calculated initial creep rate versus calculated minimum creep rate indicates a linear relationship given by:

$$CR_i = 0.0044 + 23\, MCR \tag{12}$$

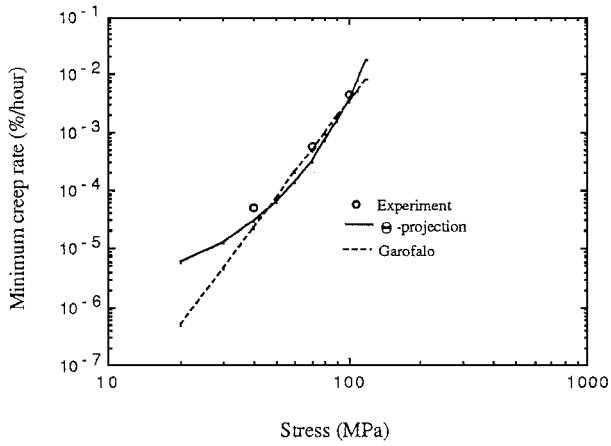

Figure 4 Experimental and predicted minimum creep rate by Θ-Projection and Garofalo models as a function of stress at 800°C.

Solving Equations 11 and 12 for $\varepsilon_t r$, and substituting into Equation 10, the creep rate, *CR,* is then found.

Variation of the creep rate constant, r, with *MCR* was also found to be generally linear with *MCR* within the investigated experimental range, expressed as:

$$r = 0.02 + 80\,MCR \tag{13}$$

Upon substituting r in the *CR* equation and then integrating, the total creep strain is found to be:

$$\varepsilon = \frac{1}{r}\left[1 - \mathrm{e}^{(-rt)}\right](0.0044 + 22\,MCR) + (MCR)t + \varepsilon_0 \tag{14}$$

where ε_0 is the instantaneous strain on loading which is zero for the creep tests of Haynes alloy 556.

According to Garofalo [10], for low stress levels Equation 7 reduces to:

$$MCR = A_3\sigma^n \tag{15}$$

where A_3 and n are constants for a given temperature. Therefore, for the investigated experimental range, Equation 9 reduces to:

$$MCR = A\sigma^n \mathrm{e}^{-Q/RT} \tag{16}$$

The constants n, Q/R and A were found by least squares fit of the experimental data, resulting in:

$$MCR = 1.18 \times 10^{-5}\sigma^{5.432}\mathrm{e}^{-20{,}850/T} \tag{17}$$

The experimental and calculated minimum creep rate data by Garofalo model versus stress and temperature are also listed in Table V. The creep curves can be constructed for the various stress and temperature conditions by using Equations 13, 14 and 17. Fig. 4 also shows predicted creep curves based on Garofalo model for stresses ranging from 40 MPa to 100 MPa, and temperatures between 760°C and 871°C.

3.3. Comparison of models with experimental results

The Θ-Projection method results in better predictions of rupture lives for the available experimental data, as indicated by ratios of predicted to experimental rupture lives listed in Table V. The predicted minimum creep rates based on the two models considered, are compared with the measured minimum creep rates at 800°C in Fig. 4. Either of the two models can be used to describe the minimum creep rate over the experimental stress range, reasonably well. Evans and Wilshire [6] examined minimum creep rate dependence on stress for 1/2Cr1/2Mo1/4V steel at 838°C. The predicted minimum creep rate dependence on stress for this steel was based on tests carried out at very low stresses using Θ-Projection method. The extrapolated measured rates were very close to the experimental data. In addition, the Θ-Projection method predicted the exact curvature of the experimentally determined $\log(\sigma)/\log(MCR)$ relationship observed in tests of long duration.

Fig. 3 shows the predicted creep curves based on each model superimposed with the experimental curves. As can be seen, the Θ-Projection method gives the best fit and representation of the experimental curves. Moreover, the Θ-Projection method provides a concise and convenient means of quantifying the entire creep characteristics of the alloy in a manner which describes the variation in creep curve with changes in stress and temperature within the experimental range. The relative extent of the primary creep stage diminishes, while the tertiary stage becomes more pronounced with decreasing stress and temperature, as predicted by the two models considered. It should also be noted that the *MCR* occurs at a progressively earlier fraction of the total life, as the stress and temperature are decreased.

The decrease in the creep exponent, n, from high values at high stresses to low values at low stresses, is usually explained by the assumption of changes in the creep mechanism. The Θ-Projection method gives an accurate prediction of the decrease in the slope of $\log(\sigma)/\log(MCR)$ relation on the basis of changes in creep curve shape, rather than changes in the creep mechanism with stress, since creep characteristics can be interpreted directly from the stress and temperature dependence of Θ_i constants. It should, however, be noted that as a function of temperature, the creep mechanism changes from obstacle-controlled dislocation glide at low and intermediate temperatures, to dislocation climb mechanism at higher temperatures [11].

The Θ-Projection method, when applied to predict the long-term creep performance, fits the primary stage very well. Some divergence from the experimental curve is seen after the point of minimum creep rate is reached, as can be seen from Fig. 3. The creep strain calculated by the Θ-Projection method consists of primary and tertiary creep strains. The primary strain rate diminishes with time, while the tertiary strain rate becomes more pronounced. Therefore, immediately after reaching the point of minimum creep rate, the net strain rate increases more rapidly without showing any region of secondary creep rate. This can explain the increase in divergence of the predicted and experimental curves with time, as seen in Fig. 3.

The lack of accuracy in Garofalo model in fitting the shape of the creep curve and predicting rupture lives is due to the fact that the model does not take into consideration the transient part of the creep curve. Therefore, predicted rupture life is much longer than

the experimental life, especially for long life situations. This model is good to be used for short life situations to calculate rupture lives.

4. Monotonic stress-strain behavior

Materials strength properties needed for calculating the allowable stresses and deflections are usually determined from stress-strain curves. Based on the time independent stress-strain data at room temperature and the creep data, the stress-strain curve at different temperatures and strain rates can be obtained. For the material investigated, first the variations of modulus of elasticity, strain hardening exponent, and strain hardening coefficient with temperature are determined. Using this information, the stress-strain curve could be obtained with varying temperatures, but at a fixed strain rate. The stress-strain curves at slow-strain-rate are then constructed by combining the time independent stress-strain data with the time dependent creep rate data, using a time incremental method.

4.1. Standard tensile tests

Data from five standard tensile tests at high temperatures were available [4]. Typical data from these tests are given in Table II. A Holloman type equation (Equation 3) is used to predict the stress-strain behavior for a given temperature.

As can be seen from Fig. 5, modulus of elasticity of Haynes alloy 556 varies linearly with temperature, and can be expressed by:

$$E = 203 - 0.073T \tag{18}$$

where T is the temperature in °C, and E is in GPa. This figure shows that modulus of elasticity decreases from 201 GPa at room temperature to 138 GPa at 900°C. This is due to the fact that the separation distance between atoms increases with temperature due to expansion from heating.

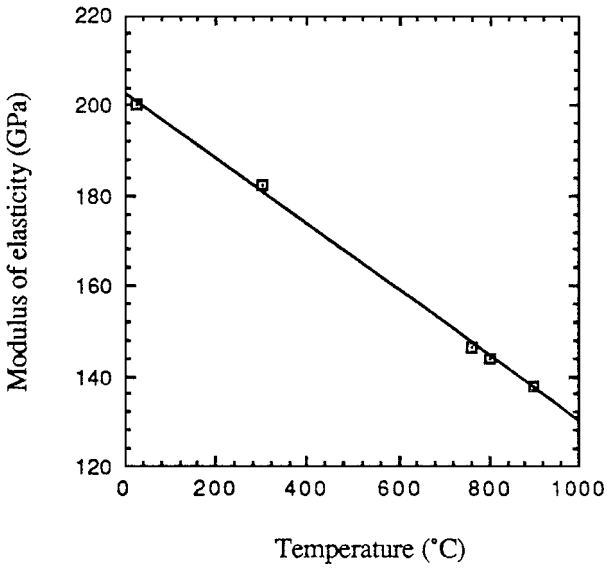

Figure 5 Temperature dependence of modulus of elasticity from standard tensile tests.

The strain hardening exponent is defined as a measure of the increase in strength of the material due to plastic deformation. Smith [12] determined the variations of the strain hardening exponent with temperature for several materials including alloy steels, copper and pure iron. For copper, he found that the strain hardening exponent decreases linearly with temperature for temperatures between 0°C and 500°C. For alloy 304 steel, the strain-hardening exponent also decreases slowly with temperature up to 600°C, and then it decreases rapidly with temperature after 600°C. For pure iron, the strain hardening exponent increases linearly with a slow rate until 400°C, then it decreases very rapidly after reaching a peak at 400°C. Therefore, there is no defined trend for the variation of the strain hardening exponent with temperature and the relationship varies from one material to another.

Plots of strain hardening exponent, n, and the strength coefficient, K, for the Haynes alloy 556 as a function of temperature are shown in Fig. 6. As can be seen in Fig. 6a, the strain hardening exponent, n, increases gradually with temperature until reaching a maximum at around 300°C, then it decreases after 300°C. This type of variation can be represented using a parabolic equation, the constants of which were determined by least squares fit as follows:

$$n = 0.1058 + 2.3 \times 10^{-4}T - 3.5 \times 10^{-7}T^2 \tag{19}$$

The strength coefficient, K, variation with temperature is modeled linearly, as shown in Fig. 6b. The strength coefficient changes with temperature in the same manner as the yield and ultimate strengths. As the temperature increases, the material becomes more ductile and the stress required to attain 100% true strain becomes smaller. A regression line through the experimental data in Fig. 6b gives:

$$K = 422 - 0.248T \tag{20}$$

where K is in MPa.

Fig. 7 shows a plot of experimental and predicted standard stress-strain curves based on Equations 3 and 18–20 for temperatures between room temperature and 900°C. As can be seen, the predictions are reasonable, particularly in the plastic strain dominated regime.

4.2. Slow-strain rate tensile response predictions

Slow-strain-rate tensile tests are used to predict the stress-strain response of Haynes alloy 556 at slow-strain-rates. Data from these tests, as listed in Table III, are used as an evaluation of how well the stress-strain response can be predicted using time-dependant tensile curves and time dependent minimum creep data.

An incremental time method was used to predict the stress-strain curves at a strain rate of 0.5%/hour, since experimental data for Haynes alloy 556 was available at this strain rate. For each time increment, the stress was assumed to be constant. The strain decrement due to

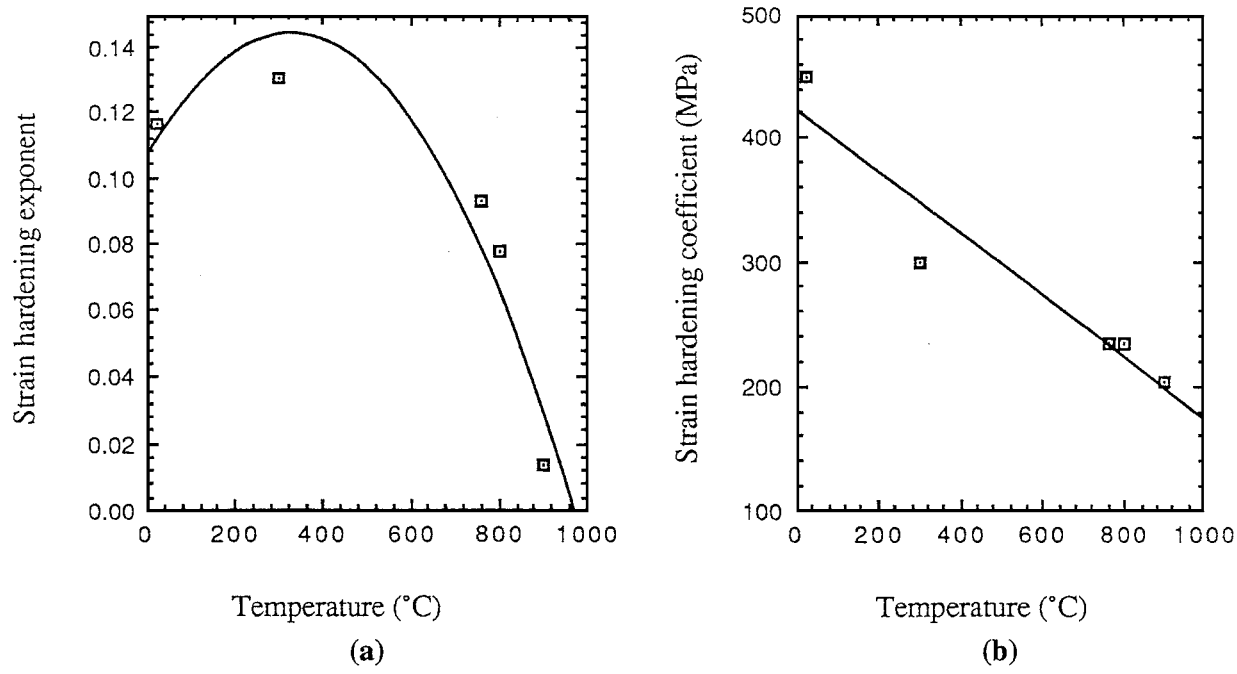

Figure 6 Temperature dependence of strain hardening exponent and coefficient.

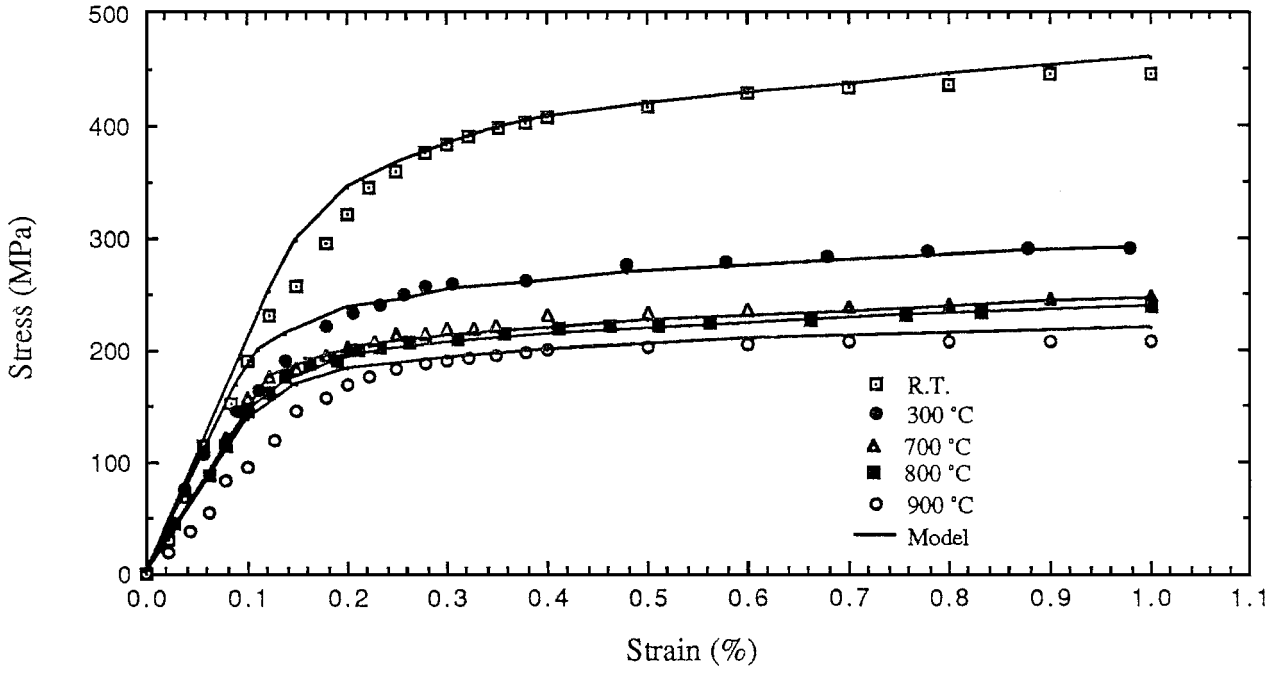

Figure 7 Tensile stress-strain curves for various temperatures showing experimental data versus curves derived from the empirical model.

creep is computed by multiplying the minimum creep rate at a given stress and temperature by the time increment. Then, the net strain is incremental strain minus the creep strain. The stress increment was determined by multiplying the net strain increment by the secant modulus. The secant modulus is calculated at the same stress used to calculate the creep strain decrement by taking the derivative of Equation 3 with respect to stress, σ. Marching on time while summing the stress and strain increments, the stress-strain curves are then constructed.

Fig. 8 shows the experimental and predicted stress-strain curves at a strain rate of 0.5% for temperatures of 23°C, 316°C, 760°C and 871°C. The curve is underestimated at room temperature. At this temperature, the stress decrement due to creep is the major factor in underestimating the calculated stress due to the fact that at room temperature the material strain hardened the most. Therefore, to gain more accuracy at room temperature, the creep effect can be neglected. At 316°C and 760°C, there is a reasonably good agreement between the experimental and calculated stress-strain curves, since there is a balance between the hardening and relaxation processes. On the other hand, at 871°C the predicted curve is overestimated, since the balance between hardening and relaxation processes is shifted toward more relaxation. Therefore, at high temperatures (871°C), to predict the curves with more

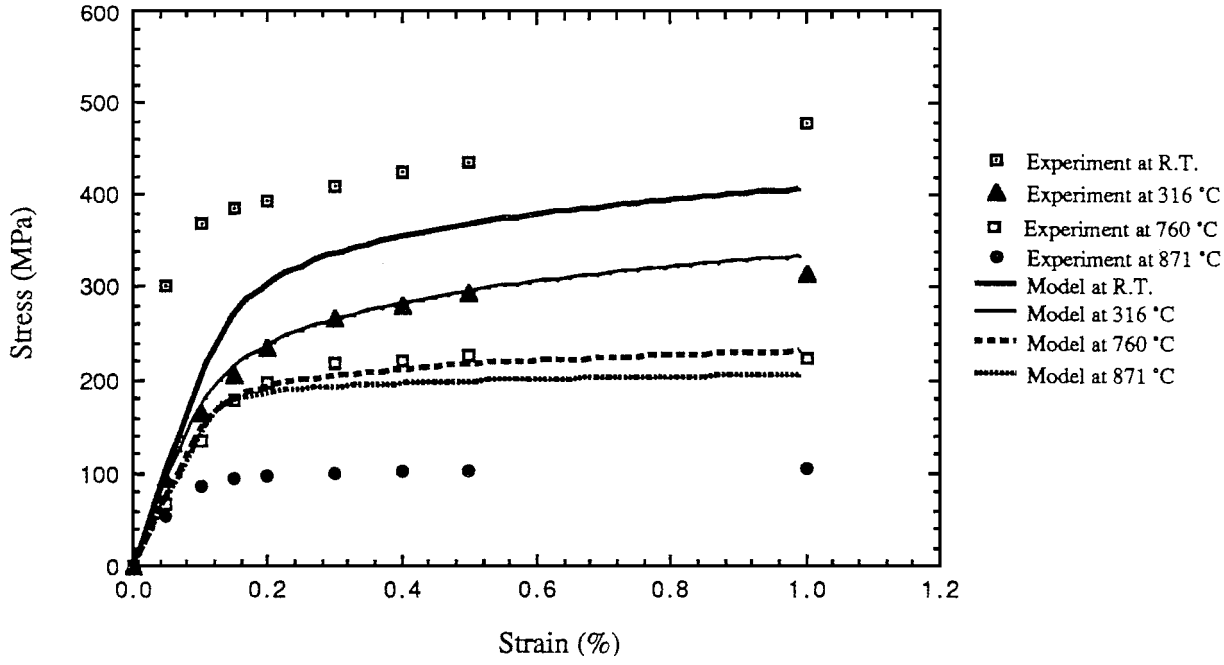

Figure 8 Experimental and predicted stress-strain response based on the time incremental method at a slow-strain-rate of 0.5%/hour.

accuracy, another stress decrement is needed to account for relaxation. To accomplish this task, more relaxation experiments are needed at various temperatures.

5. Conclusions

Based on the analysis and discussion of the experimental data and models presented, the following conclusions can be made:

1. For the Haynes alloy 556 investigated, the strain-time curve at any stress and temperature within the ranges studied can be constructed using either the Θ-Projection or the Garofalo model. The Θ-Projection model for creep deformation predicts the variation in creep curve curvature as a function of temperature and stress level reasonably well. Moreover, this model gives more accurate prediction for the rupture life than Garofalo model within the experimental range.

2. Both Θ-Projection and Garofalo creep models can reasonably predict the minimum creep rate as a function of stress for a given temperature. However, the creep exponent, n, does not vary with stress for a given temperature according to Garofalo model, but rather, it decreases from high values at high stresses to low values at low stresses according to the Θ-Projection model.

3. Modulus of elasticity of Haynes alloy 556 decreases linearly as the temperature increases in the range of experimental data. The strain hardening exponent varies parabolically with temperature, while the strain hardening coefficient decreases rather linearly with temperature in the range of experimental data.

4. The stress-strain prediction model based on the incremental time method gives reasonable predictions at intermediate temperatures (316°C and 760°C). The stress-strain curves are underestimated at room temperature, and overestimated at the highest test temperature (871°C).

Acknowledgements

The data used in this work were generated at the Oak Ridge National Laboratory (ORNL) by T. H. Krukemyer during his graduate studies at the University of Toledo. Appreciation is expressed to R. W. Swindeman of the Metals and Ceramics Division at ORNL for managing this activity.

References

1. R. VISWANATHAN, "Damage Mechanisms and Life Assessment of High Temperature Components" (ASM International, Metals Park, Ohio, 1989).
2. S. G. R. BROWN, in Proceedings of the Third International Conference on Creep and Fracture of Engineering Materials and Structures, 1987, p. 829.
3. Haynes International, "Haynes Alloy No. 556," Catalog No. H 3013, Kokomo, IN, 1986.
4. T. H. KRUKEMYER, Master thesis, Department of Mechanical Engineering, The University of Toledo, Toledo, Ohio, August 1991.
5. T. H. KRUKEMYER, A. FATEMI and R. W. SWINDEMAN *ASME Journal of Engineering Materials and Technology* **116** (1994) 54.
6. R. W. EVANS and B. WILSHIRE, "Creep of Metals and Alloys," The Institute of Metals, London, 1985 p. 197.
7. K. MARUYAMA and H. OIKAWA, in International Creep Conference, 1987, p. 815.
8. R. VISWANATHAN, *Metallurgical Transactions* **8A** (1977) 877.
9. F. GAROFALO, "Fundamentals of Creep and Creep-Rupture in Metals" (McMillan Company, New York, 1965) p. 46.
10. *Idem.*, *Transactions of the Metallurgical Society of AIME* **227** (1963) 351.
11. A. D. FREED, S. V. RAJ and K. P. WALKER, *ASME Journal of Engineering Materials and Technology* **114** (1992) 46.
12. G. V. SMITH, "The Application of Elevated Temperature Yield Strength and Code Allowable Stresses" (The American Society of Engineers, New York, 1974) p. 157.

Received 30 July 2001
and accepted 27 March 2002